Regular Article

ORGANIC CHEMISTRY RESEARCH
Published by the
Iranian Chemical Society
www.orgchemres.org

Org. Chem. Res., *Vol. 2, No. 2, 102-112, September 2016.*

Computational Chemistry of Anthracene (PAH) Removal by SWNT Nano-filters: DFT

L. Mahdavian*

Department of Chemistry, Doroud Branch, Islamic Azad University, P.O. Box: 133. Doroud. Iran

(Received 23 September 2015, Accepted 5 February 2016)

Polycyclic aromatic hydrocarbons (such as, anthracene, benzo[a]pyrene and so on) are non-polar, hydrophobic compounds, which are not ionized. They are only slightly soluble in water. They are very dangerous compounds in the environment. The single-walled carbon nanotube (SWNT) is used for removal and conversion of anthracene to low-risk products. In this study, electron transfer between anthracene and SWNT (8,8) is evaluated through density functional approach at the level of B3LYP/6-31G. The calculation of the electronic properties shows that SWNT is very sensitive to the presence of anthracene molecule. The HOMO/LUMO and gap energy (E_g) changes were considerable. According to the calculated thermodynamic parameters through the DFT method, it is expected that SWNT be a candidate in the elimination of anthracene as well as a gas sensor for its detection and conversion. Regarding the thermodynamic results, the absorption of pollutant on nano-surface of SWNT is exothermic and spontaneous. The results show that the pollutant can be reduced or eliminated from the environment by single-walled carbon nanotubes.

Keywords: Polycyclic aromatic hydrocarbons (PAHs), SWNT (8,8), Density of states (DOSs), Computational methods

INTRODUCTION

Polycyclic aromatic hydrocarbons (PAHs) are a group of over 100 different chemicals that are formed during the incomplete burning of coal, oil and gas, garbage, or other organic substances like tobacco or charbroiled meat, however a few of PAHs are used in producing medicines, dyes, plastics, and pesticides [1,2]. The increase in the rate of lung cancer has been attributed to polycyclic aromatic hydrocarbons [3,4]. Anthracene ($C_{14}H_{10}$), a solid PAH consisting of three benzene rings derived from coal-tar, is the simplest tricyclic aromatic hydrocarbon (also called Para naphthalene or green oil). It is on the EPA's priority pollutant list. It is ubiquitous in the environment as a product of incomplete combustion of fossil fuels. It has been identified in surface and drinking water, ambient air, exhaust emissions, the smoke of cigarettes and cigars, and in smoked foods and edible aquatic organisms [5,6].

There are some methods to eliminate pollutants from the environment such as decomposing by bacteria (Geobacillus) [7,8], using earthworm of Eisenia Fetida [9], phytoremediation [10,11], using Zeolite [12] and so on. Over the last decade, single-walled carbon nanotubes (SWNTs) have been used to reduce and remove organic pollutants from the environment [13,14]. SWNTs are also effective sorbents for organic chemicals [15] such as trihalomethanes [15], naphthalene [16] polar and nonpolar aliphatic and polycyclic aromatic hydrocarbons (PAHs) due to their hydrophobic graphene surfaces [13] and π-π stacking strong interactions between aromatic compounds and SWNTs. In the present study, SWNTs were simulated and studied to recognize, eliminate, and change polycyclic aromatic hydrocarbons (Anthracene) into less dangerous compositions. Also, carbon nanotube sensors have a potential capability for the monitoring in environment and can be easily developed for poisons and harmful chemicals [17].

*Corresponding author. E-mail: Mahdavian@iau-doroud.ac.ir

COMPUTATIONAL METHODS

The primary structures of single-walled nanotube (SWNT) were optimized in length and diameter by nanotube modeler software. The calculation was performed for an armchair (8,8) model of nanotube with 11.28 Å length and 10.88 Å diameter. The carbon atoms situated at both ends of this length have a negative charge because of carbon bond breaking. For saturation of the carbon bond in the two ends of the nano wire and create a model similar to a real wire of nanotube, hydrogen atoms were added to the end links of nanotube, as shown in Fig. 1.

The SWNT (8,8) and anthracene were optimized by Gaussian program package, with B3LYP functional and 6-31G basis set (Fig. 1). There are three situations for the absorption of pollutants on SWNT: 1-passing of anthracene from a central axis, 2-adsorption at the end of SWNT and 3-adsorption of anthracene on the wall of SWNT. The adsorption of anthracene is simulated, and consequently, the electrical and thermodynamic properties of the interaction are studied. Computation can be carried out for the systems in the gas phase or solution state, in ground or excited state.

Gaussian provides a wide range of functionals to predict the right energies, decomposition components and decomposition frequencies computable for all DFT models [18,19].

To examine thermodynamic properties of chemical phases, semi empirical computation was carried out. The thermodynamic energy (E_{th} (kcal mol^{-1})) has been calculated as follows:

$$E_{th} = E_{Anthracene\text{-}SWNT} - [E_{Anthracene} + E_{SWNT} + \delta_{BSSE}] \quad (1)$$

where $E_{Anthracene\text{-}SWNT}$ is the adsorption energy of the anthracene-SWNT complex, E_{SWNT} is the adsorption energy of the SWNT, $E_{Anthracene}$ represents the energy of an isolated anthracene molecule and δ_{BSSE} is the basis set superposition error.

RESULTS AND DISCUSSION

PAHs are stable and low biodegradable compounds [18]. In this study, the interaction and adsorption of anthracene on SWNT are investigated (8,8). This interaction is carried out in vacuum for the removal of the effect of all environmental factors. Generally chosen for the production of a specific product, is also of interest in computational chemistry. Therefore, computational methods have been employed to gain significant insight into the chemical processes which are not comprehensible through common laboratory settings [19].

The Anthracene Passing into SWNT

At first, the Z-matrix files of SWNT (8,8) and anthracene were produced, and then corresponding structures were optimized at the level of B3LYP/6-31G embedded in Gaussian software working under Linux. Next, the anthracene passing through the central axis of the nanotube was simulated at five steps. Figure 2 shows the stick model of the optimized structure for this transfer and adsorption by DFT. The anthracene passing from SWNT is

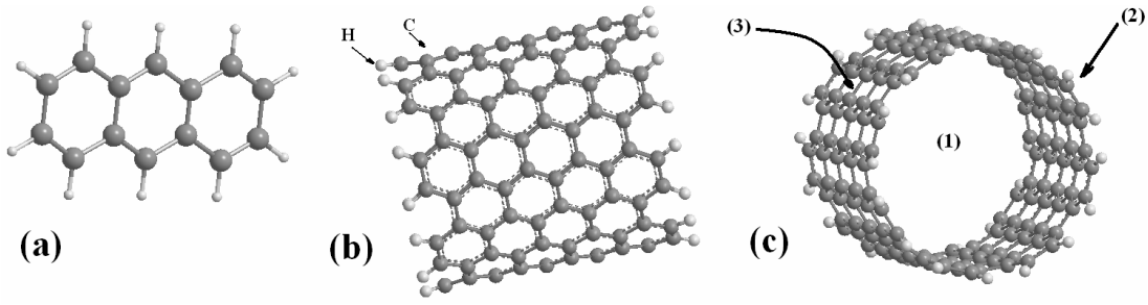

Fig. 1. The optimized geometrical structure of: a) anthracene, b) single-walled carbon nanotube (8,8) and c) situations of anthracene absorption on SWNT.

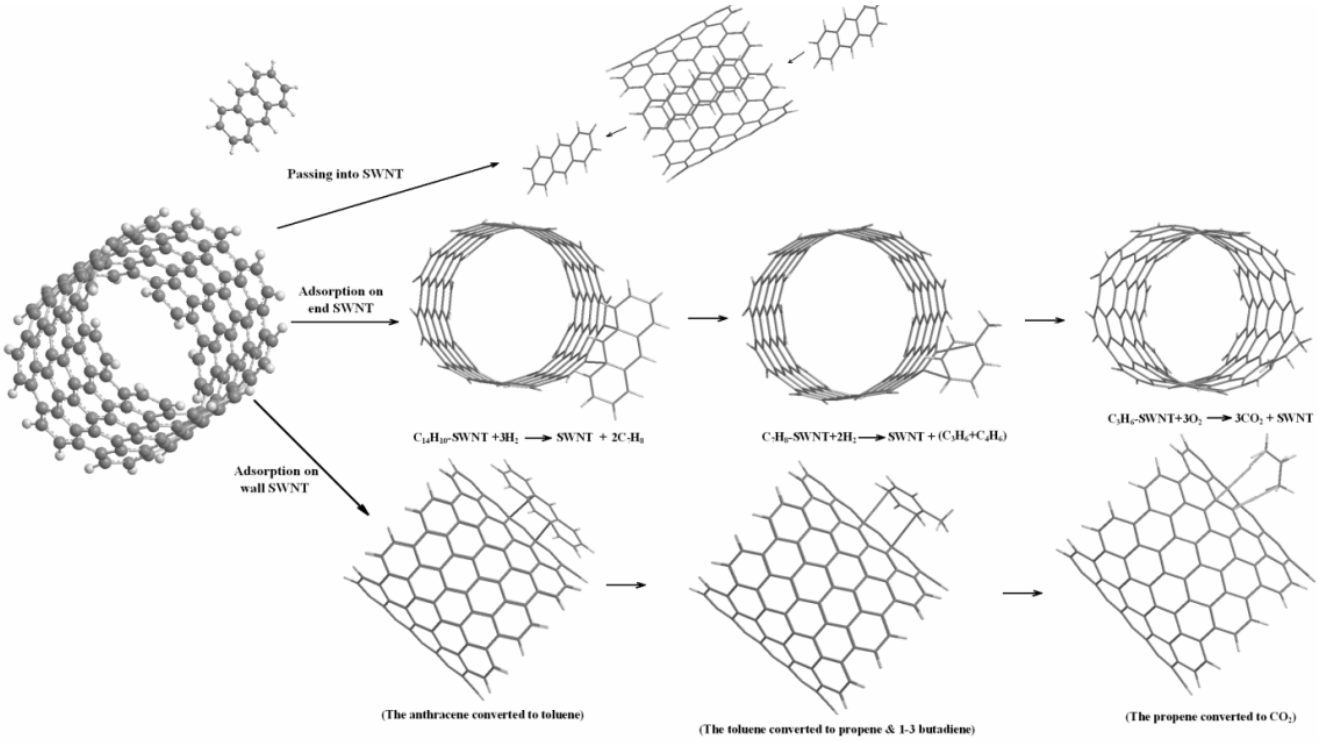

Fig. 2. Ball-and-stick model configuration of anthracene passing into and adsorption on the SWNT (8,8).

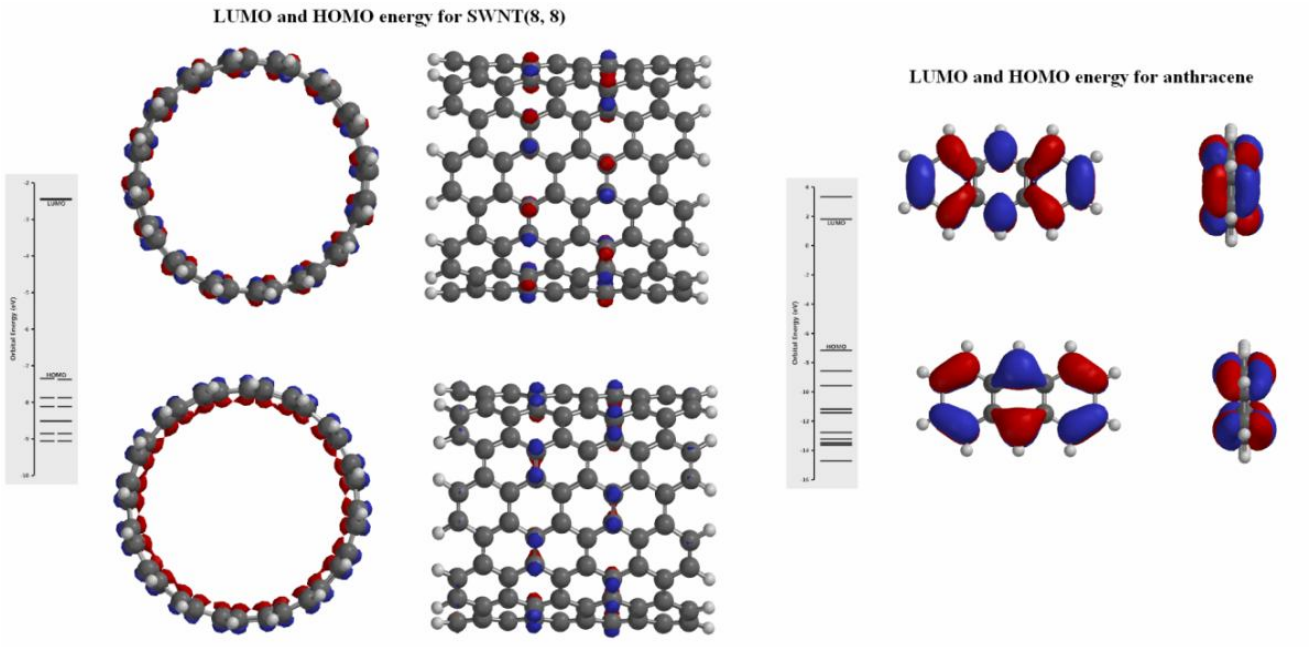

Fig. 3. The computed molecular electrostatic potential surfaces for SWNT (8,8) and anthracene.

simulated in five steps; at first, anthracene is placed along the central axis of nanotube, in the second step, it is entered into the nanotube and in the third step, it reaches to the center. The thermodynamic properties, and obtained results containing the density of states (DOSs) are shown in Table 1. The thermodynamic properties and DOS of this interaction, shown in Fig. 3, were computed at the B3LYP/6-31G level. As a pollutant enters into the nanotube, dipole moment (D) decreases, indicating that electronic charge on SWNT atoms decrease and the root mean squared (RMS) gradient (kcal mol^{-1} $\mathbf{Å^{-1}}$) is computed for all steps by this method. RMS gradient is maximum in the 3rd and 4th steps. As the adsorption energy in the center of the nanotube (4144182 kcal mol^{-1}) decreases compared to that of the previous step (4162672 kcal mol^{-1}) entrance of pollutant to nanotube becomes exothermic and spontaneous.

The DOS is often used for quicker visual analysis of the electronic structure. Characteristics such as the width of the

Table 1. The Thermodynamic and Electronic Properties of Anthracene Passing into SWNT (8,8) with 11.01 Å Length at 298 K (B3LYP/6-31G)

	E_{ad} (kcal mol^{-1})	Dipole moment (D)	RMS (Kcal mol^{-1} $Å^{-1}$)	E_{bin} (kcal mol^{-1})	H (kcal mol^{-1})	G_{ele} (kcal mol^{-1})	E_{ele} (kV)	E_{nuc} (kcal mol^{-1})
Anthracene	-44488.5	0.1	29.4	-2838.6	74.8	-254868.1	-11.1	210379.6
SWNT (8,8)	2023061.9	10550	3776	2467681.7	2495024.1	-7463247.5	-324.8	9486309.4
Steps	E_{ad} (kcal mol^{-1})	Dipole moment (D)	RMS (Kcal mol^{-1} $Å^{-1}$)	E_{bin} (kcal mol^{-1})	H (kcal mol^{-1})	G_{elec} (kcal mol^{-1})	E_{elec} (kV)	E_{nuc} (kcal mol^{-1})
1	3911170	12100	3840	-45976.9	-45976.9	-1242327	-54.1	1196350
2	4162672	10900	3844	205525.0	205525.0	-1566920	-68.2	1772445
3	4144182	10800	4025	287035.2	287035.2	-1817019	-79.1	2104054
4	4194345	10900	4062	237198.2	237198.2	-1728786	-75.2	1965984
5	3911081	12100	3840	-45966.9	-45875.9	-1242827	-54.1	1196790
	E_{LUMO} (eV)	E_{HOMO} (eV)	E_g (eV)	μ (eV)	η (eV)	Σ (eV)	Ω (eV)	S (eV)	ΔN_{MAX} (eV)
Anthracene	1.811	-7.161	8.971	-2.675	4.485	-3.485	16.046	0.111	0.596
SWNT (8,8)	-2.460	-7.350	4.891	-4.905	2.445	-1.445	29.412	0.204	2.006
1	-2.812	-6.985	4.173	-4.899	2.087	-1.087	25.036	0.241	2.348
2	-2.811	-7.047	4.235	-4.929	2.118	-1.118	25.727	0.236	2.328
3	-2.807	-7.179	4.372	-4.993	2.186	-1.186	27.248	0.229	2.284
4	-2.809	-7.289	4.481	-5.049	2.240	-1.240	28.561	0.223	2.254
5	-2.811	-7.005	4.194	-4.908	2.097	-1.097	25.260	0.238	2.342

valence band, the gap energy in insulators and the number and intensity of the main features are helpful in qualitatively interpreting experimental spectroscopic data. Table 1 shows DOS parameters including E_{LUMO} (energy of the lowest unoccupied molecular orbital), E_{HOMO} (energy of the highest occupied molecular orbital), E_g (gap energy), μ (chemical potential or negative of electronegativity), η (chemical hardness), σ (chemical softness), ω (electrophilicity), S (global softness) and ΔN_{MAX} (charge transfer in molecules) [19,20].

$$\mu = (E_{LUMO} + E_{HOMO})/2 \quad (2)$$

$$\eta = (E_{LUMO} - E_{HOMO})/2 \quad (3)$$

$$\sigma = 1 - \eta \quad (4)$$

$$\omega = \mu^2/2\eta \quad (5)$$

$$S = 1/2\eta \quad (6)$$

$$\Delta N_{MAX} = -\mu/\eta \quad (7)$$

The gap energy (E_g) is a major factor for the determination of the electrical conductivity of nanotubes. If the calculated amount of E_g for the complexes is low, sensitivity and conductivity of absorbent surface will be considerable and nanostructure can be used as nano adsorbent. In studying interactions, the maximum amount of gap energy has been occurring in the 3rd and 4th steps. As is shown in Table 1, E_g for the 3rd and 4th steps are 4.372 and 4.481 eV, respectively.

According to Table 1, the chemical potential (μ) decreases in the 3rd and 4th steps indicating electron transfer from SWNT to anthracene. The chemical hardness (η) and chemical softness (σ) are used for evaluation of the hardness and softness of molecules. Hard molecule has a large HOMO-LUMO gap while a soft molecule has a small HOMO-LUMO gap [21]; therefor, the 3rd and 4th steps are harder than other states and can easily change their electron density. The electrophilicity (ω) is a measure of the electrophilic power of a molecule. The ω value increases in these steps, showing their higher electrophilicity. So, it is a stronger Lewis acid. The global softness, S, of the equilibrium state of an electronic system at temperature T is defined by a sudden change in thermodynamic properties which takes place when anthracene is desorbed. In addition, the amount of charge transferred can be calculated by the maximum amount of electronic charge (ΔN_{MAX}). The $\Delta N_{MAX} > o$ indicates the molecule acts as an electron acceptor [21].

The same changes can be seen in the enthalpy of formation (H). The binding energy (E_{bin}) and the nucleic energy (E_{nuc}) increase compared to those in the previous step, while the Gibbs free energy (G_{elec}) decreases. The electrical properties of carbon nanotube, the electric energy E_{elec}/kV, decreases as anthracene enters into the tube. This increases electric resistance of nanotube. Changes in electric resistance in all steps can be seen in Fig. 4. As shown in Fig. 4, crossing anthracene through the tubes is accompanied by conductivity enhancement and maximum changes can be seen in the 3rd step. The observed changes in electrical properties show, SWNT (8,8) are able to detect anthracene. The electrical resistance is calculated by the conductivity as:

$$E_{elec} = RI \quad (8)$$

where I (A) is electrical intensity, R (Ω) is electrical resistance and E_{elec} (V) is electrical energy. Following equation is used to calculate R:

$$R = \frac{E_{ele}\, t}{n.\mathrm{F}} \quad (9)$$

where n, F and t are the number of electrons exchanged, Faraday's constant and time (h) of interaction, respectively. The electrical resistance- time graph was drawn from the information of Table 1 and Eqs. (8) and (9).

Table 2 shows temperature changes in the center of carbon nanotube (8,8). As temperature increases, thermodynamic parameters rise. In 423 K, the total energy and other parameters decrease. This shows that after absorption of pollutant by carbon nanotube, it can be removed and recycled by the rise of temperature.

Anthracene Absorption on SWNT (8,8)

The SWNT sensitivity to aromatic organic compound is

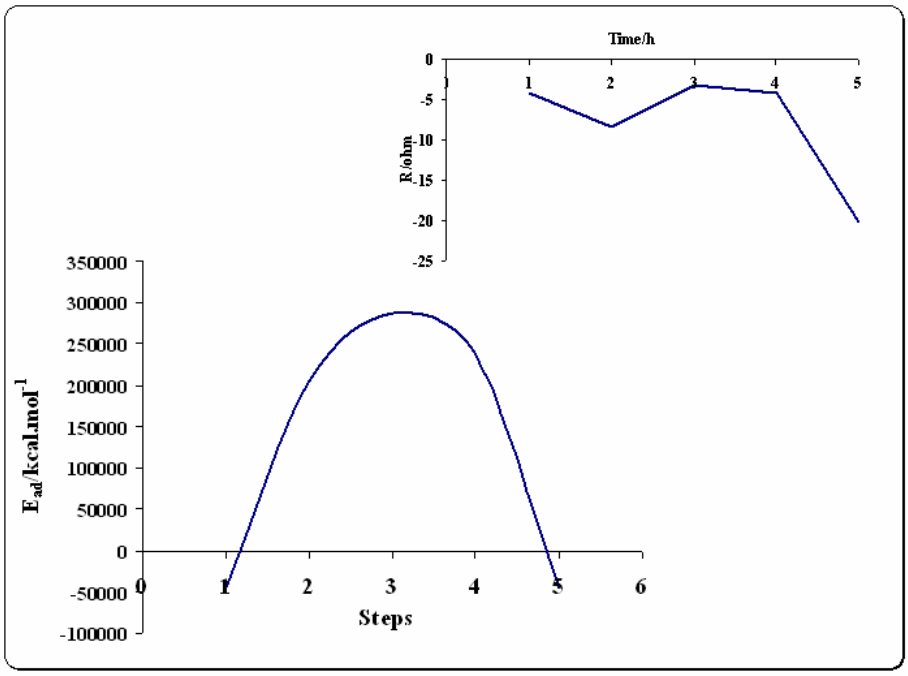

Fig. 4. The adsorption energy (kcal mol^{-1}) and the electric resistance (Ω) of anthracene passing into SWNT (8,8) at 298K (B3LYP/6-31G).

Table 2. The Effect of Temperature on Anthrancene in the 3rd Step in the Center of SWNT (8,8)

T (K)	E_{ad} (kcal mol^{-1})	Dipole moment (D)	RMS (Kcal mol^{-1} Å^{-1})	E_{bin} (kcal mol^{-1})	H (kcal mol^{-1})	G_{ele} (kcal mol^{-1})	E_{ele} (kV)	E_{nuc} (kcal mol^{-1})
298	3911170	10800	4025	287035.2	287035.2	-1817019	-79.1	2104054
323	3911245	10800	4025	287984.1	287223.4	-2145632	-79.1	2104055
373	3911261	10800	4025	288513.4	287624.1	-1606893	-79.0	2104056
423	3802568	10800	4025	286006.8	282196.6	-2769382	-79.3	2104057

investigated in the current study. When anthracene is exposed to carbon nanotube, one possibility is that the pollutant is absorbed at the end or on the wall of carbon nanotube. The exchange of electron between them can change anthracene into less risky products. In this study, anthracene absorption at the end or tip of SWNT was simulated and their geometric structure was optimized (Fig. 2). After absorption, anthracene will change into other products based on the following mechanisms.

$C_{14}H_{10}$-SWNT + $3H_2 \rightarrow 2C_7H_8$ + SWNT
(The anthracene converted to toluene)

C_7H_8-SWNT + $2H_2 \rightarrow (C_3H_6 + C_4H_6)$ + SWNT
(The toluene converted to propene & 1-3 butadiene)

Table 3. The Thermodynamic Properties of Anthracene Adsorption at the End and on the Wall of SWNT (8,8) at 298 K (B3LYP/6-31G Method)

Steps	E_{ad} (kcal mol^{-1})	Dipole moment (D)	RMS (Kcal mol^{-1} $Å^{-1}$)	E_{bin} (kcal mol^{-1})	H (kcal mol^{-1})	G_{ele} (kcal mol^{-1})	E_{ele} (kV)	E_{nuc} (kcal mol^{-1})
Anthracene	-44488.5	0.1	29.4	-2838.6	74.8	-254868.1	-11.1	210379.6
SWNT (8,8)	2023061.9	10550	3776	2467681.7	2495024.1	-7463247.5	-324.8	9486309.4
$C_{14}H_{10}$-SWNT $+3H_2 \rightarrow 2C_7H_8$ + SWNT (anthracene converted to toluene)								
The adsorption on the end of SWNT								
1	-1969835	13920	3588	-2454062	-2484191	7682889	0.183	-9652725
2	-1969604	10540	3541	-2453831	-2483960	7682021	0.187	-9651625
3	-1967784	12890	3973	-2452012	-2482141	7682130	0.186	-9649914
4	-1968541	12570	3836	-2452766	-2482895	7681163	0.191	-9649704
5	-1968687	12610	3634	-2452908	-2483035	7682065	0.187	-9650753
The adsorption on the wall of SWNT								
1	-1967986	14270	3937	-2452213	-2482342	7683172	0.181	45867.01
2	-1969837	12400	3926	-2454064	-2484193	7680113	0.197	47074.97
3	-1966986	12960	4324	-2451213	-2481342	7681949	0.187	48090.62
4	-1967293	12710	4277	-2451522	-2481652	7681929	0.187	47803.13
5	-1967140	13530	4183	-2451361	-2481488	7681883	0.188	48002.21
C_7H_8-SWNT$+2H_2 \rightarrow (C_3H_6+C_4H_6)$ + SWNT (The toluene converted to propene & 1-3 butadiene)								
The adsorption on the end of SWNT								
1	-1969345	11960	3819	-2453666	-2483802	7685420	0.169	-9654765
2	-1969252	11740	3777	-2453573	-2483709	7685215	0.17	-9654467
3	-1969526	10910	3830	-2453838	-2483972	7683865	0.177	-9653392
4	-1971065	10810	3935	-2455372	-2485505	7681913	0.188	-9652978
5	-1969191	12410	3699	-2453498	-2483631	7684629	0.174	-9653820
The adsorption on the wall of SWNT								
1	-1968941	12730	3671	-2453253	-2483387	7684983	0.172	43100.52

Table 3. Continued

2	-1968676	12270	3757	-2452987	-2483121	7684605	0.174	43744.44
3	-1968541	12200	3982	-2452852	-2482986	7684550	0.174	43934.61
4	-1968496	12160	3966	-2452807	-2482940	7684119	0.176	44405.71
5	-1968977	12780	3802	-2453284	-2483418	7684716	0.173	43331.68
C_3H_6-SWNT+$3O_2 \rightarrow 3CO_2$ + SWNT (The propene converted to CO_2)								
The adsorption on the end SWNT								
1	-1969345	0.1152	42.19	-2464950	-2495087	7674860	0.224	-9655449
2	-1969252	0.1458	42.19	-2464950	-2495087	7674745	0.225	-9655335
3	-1969526	0.7355	43.04	-2464949	-2495087	7674616	0.225	-9655205
4	-1971065	0.1026	42.98	-2464950	-2495087	7674465	0.226	-9655057
5	-1969191	1.0510	53.93	-2464949	-2495086	7671440	0.242	-9652207
The adsorption on the wall SWNT								
1	-1969661	10980	3897	-2454021	-2484159	7685719	0.168	41645.07
2	-1969256	11510	3780	-2453617	-2483754	7685904	0.167	41865.13
3	-1969287	11080	3948	-2453647	-2483785	7685512	0.169	42226.07
4	-1969465	10930	3682	-2453820	-2483957	7684943	0.172	42617.21
5	-1969034	12410	4509	-2453217	-2483354	7682102	0.187	45888.73

C_3H_6-SWNT + $3O_2 \rightarrow 3CO_2$ + SWNT
(The propene converted to CO_2)

As shown in Fig. 2, the interaction of the pollutant with the head and the wall of the nanotube and its conversion to the products are simulated. The absorption and change of each reaction (above mentioned) were computed in 5 steps. In the 1st and 2nd steps, the pollutant will approach to carbon nanotubes and will be absorbed. The 3rd step is the transition state of the reactions. In the 4th step, a new product is produced and in the 5th step, it is desorbed on the surface of carbon nanotube.

Absorption at the end and on the wall is another possibility of pollutant absorption on SWNT in Fig. 2. The mechanism of absorption and conversion on the pollutant into another product is the same as the previous possibility of absorption at the end and on the wall of nanotube. Thermodynamic parameters of anthracene conversion to other products and finally to CO_2 have been computed by the B3LYP/6-31G method as reported in Table 3.

The computed thermodynamic properties for adsorption on the wall of SWNT are different from those at the end of the nanotube, which is caused by the position of carbon nanotube and its atomic force field. Also, total energy and other forms of energy are higher for this conversion. As shown in Figs. 5 and 6, the E_{ad} of the intermediate of converting anthracene to carbon dioxide has a sudden change in the 3rd and 4th steps, which is the transition state of the product.

These changes are observed for other energy values in Table 3. The maximum RMS is achieved in the transition state. This is indicative of the decrease in polarity and

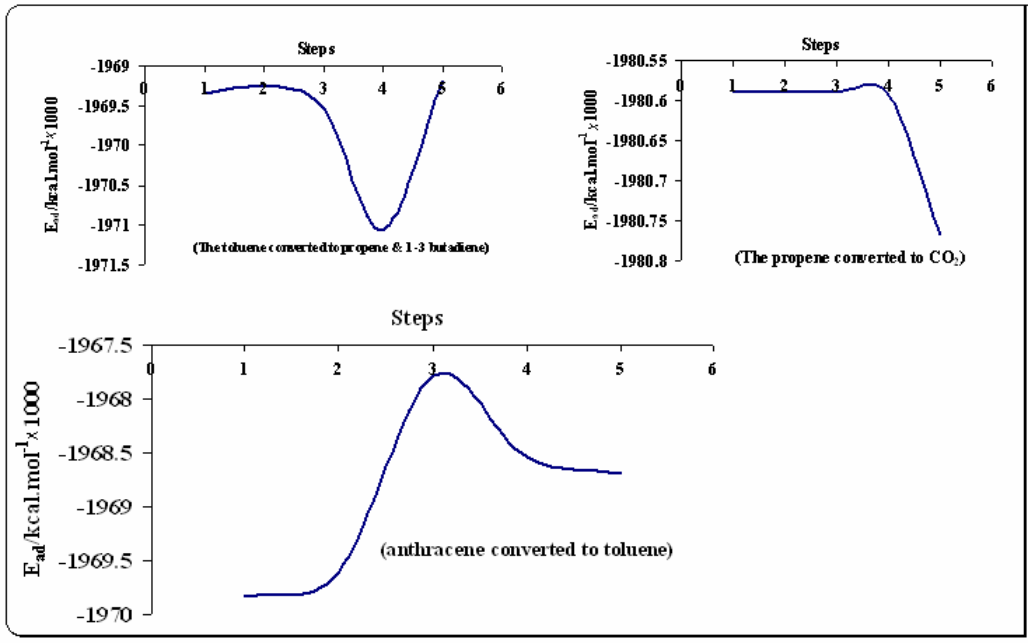

Fig. 5. The E_{ad} kcal mol^{-1} of anthracene adsorption at the end of SWNT (8,8).

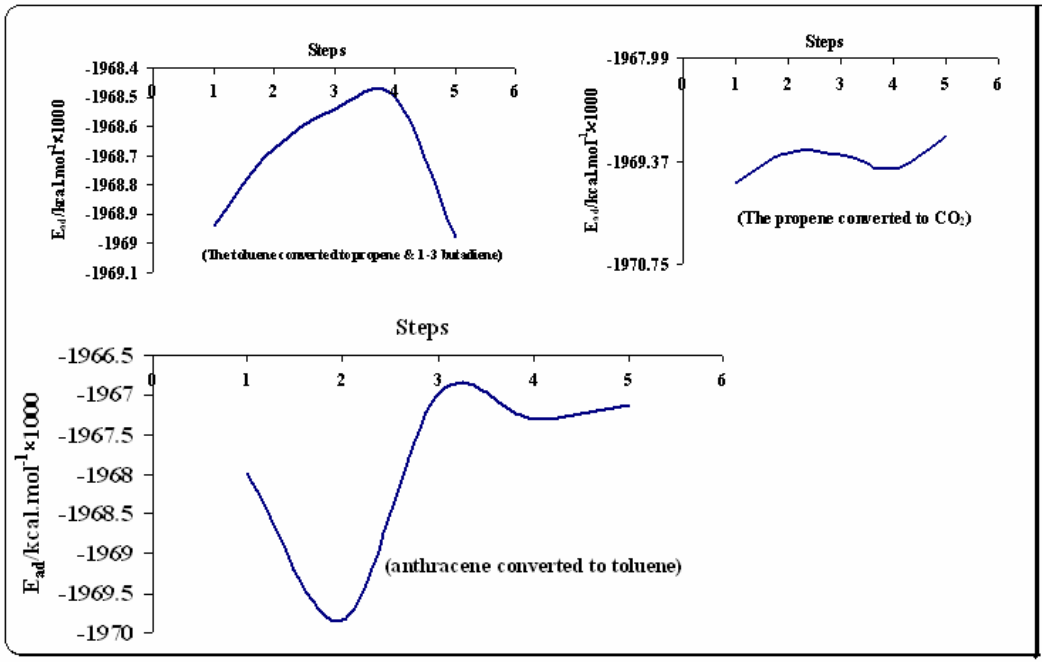

Fig. 6. The E_{ad} kcal mol^{-1} of anthracene adsorption on the wall of SWNT (8,8).

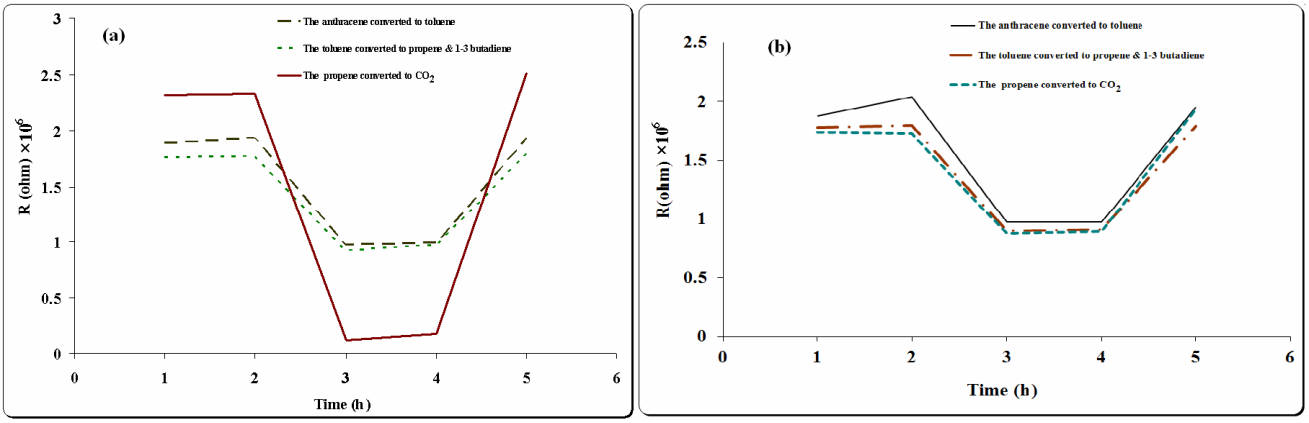

Fig. 7. The electric resistance (Ω) of anthracene adsorption : a) at the end, b) on the wall of SWNT (8,8) at 298 K (B3LYP/6-31G).

Table 4. The Thermodynamic Properties of Anthracene and SWNT (8,8) at 298 K

Reaction		ΔG_{ele} (kcal mol^{-1})	ΔH_{ele} (kcal mol^{-1})	ΔS_{ele} (kcal K^{-1} mol^{-1})	lnK
Adsorption on the end of SWNT	Anthracene to toluene	-824.01	1155.95	6.64	1396.53
	Toluene to propene & 1-3 butadiene	-790.64	170.59	3.23	1339.98
	Propene to CO_2	-3419.43	0.62	11.48	5795.25
Adsorption on the wall of SWNT	Anthracene to toluene	-1289.73	853.73	7.19	2185.84
	Toluene to propene & 1-3 butadiene	-267.36	-30.69	0.79	453.12
	Propene to CO_2	-3617.23	804.42	14.84	6130.48

electron transfer between nano surfaces with pollutant and its transition products. Also, the change in electrical properties and electric resistance for the reaction of converting propene to CO_2 is more than other forms of energy (Fig. 7).

As it is obvious in Table 3 and Fig. 7, electric energy is maximum in the 3rd and 4th steps, which are in transition and production phases. Also, the polar moment of the 4th step is maximum because of the increase in polarity and the symmetry group of the products. The electrical properties of the carbon nanotubes depend on their chirality and diameter. They can be a conductive and semi conductive. Two types of armchair and chiral are always more conductive than zigzag type and are semi conductive [13]. In this study, the conductivity of SWNT (8,8) is increased by anthracene absorption (Fig. 7).

Other thermodynamic properties of anthracene absorption and its conversion into less risky products can be seen in Table 4. The ΔG_{elec} (Gibbs free energy), ΔH_{elec} (enthalpy of formation), ΔS_{elec} (formation entropy) and lnK

(equilibrium constant) of these electronic interactions are calculated by B3LYP/6-31G.

(ΔG_{ele}) is negative, so the studied adsorption process is spontaneous. Although (ΔH_{ele}) is positive, because of the significant positive value of entropy, its effect is not remarkable within interactions. Consequently, adsorption of anthracene on armchair SWNT (8,8) is favorable in the presence of a little external heat. The adsorption on the wall of SWNT is more negative than that at the end, therefor it is more favorable.

CONCLUSIONS

The geometrical structure and electrical properties of the interaction of anthracene with SWNT (8,8) were simulated and investigated theoretically through the DFT method at the B3LYP/6-31G level. To measure the absorption sensitivity and passing of this pollutant, HOMO and LUMO energies and other parameters of the band gap were calculated. A decrease of E_g/eV indicated small excitation energy leading to the increase in complex conductivity. Calculation of DOS parameters showed transition states of the studied interactions have a softer structure (according to electrophilicity and ΔN_{MAX}), and greater chemical potential which means electron transfer between the involved species occurs easier and greater than that in the intermediate and the products. The SWNT (8,8) can be used to identify, conversion and removal of PAH compounds such as anthracene. As the findings of the study show, SWNT (8,8) can be applied to reduce and remove anthracene as a poisonous, risk factor for health of human being. The resulted thermodynamic properties show that interactions are spontaneous and exothermic. So they can be easily applied for purification of the environment.

REFERENCES

[1] M. Jiping, X. Ronghui, L. Jinhua, Y. Junbao, Z. Yanqing, C. Lingxin, J. Chromatography A 1217 (2010) 5462.

[2] O.S. Ayanda, J. Mater. Sci. 2 (2014) 14.

[3] R.R. Navarro, H. Ichikawa, Y. Iimura, K. Tatsum, Environ. Sci. Technol. 41(2007) 4240.

[4] Y. Mihoko, T. Hideshige, Pollution Bulletin. 47 (2003) 105.

[5] M.E. Khames Saad, R. Khiari, E. Elaloui, Y. Moussaoui, Arab. J. Chem. 7 (2014) 109.

[6] K. Ghosh, T. Sen, A. Patra, New J. Chem. 34 (2010) 1387.

[7] E.G. Plotnikova, O.V. Altyntenseva, Microbiology 70 (2001) 51.

[8] J. Bauer, G. Douglas, Slurries 54 (1988) 1649.

[9] E. Coutiño-González, B. Hernández-Carlos, R. Gutiérrez-Ortiz, L. Dendooven, International Biodeterioration and Biodegradation. 64 (2010) 525.

[10] J.L. Bonnet, P. Guiraud, M. Dusser, M. Kadri, J. Laffosse, R. Steiman, J. Bohatier, Ecotox Environ. Safe. 60 (2005) 87.

[11] P. Binet, J.M. Portal, C. Leyval, Org. Geochem. 32 (2001) 217.

[12] H. Sepehrian, S. Waqif-Husain, M. Ghannadi-Maragheh, 70 (2009) 277.

[13] J. Lu, S. Nagase, X. Zhang, D. Wang, M. Ni, Y. Maeda, O.T. Wakahara, T. Nakahodo, T. Tsuchiya, T. Akasaka, Z. Gao, D. Yu, H. Ye, W.N. Mei Y. Zhou, J. Am. Chem. Soc. 128 (2006) 5114.

[14] T.P. Ahammed Shabeer, A. Saha, V.T. Gajbhiye, S. Gupta, K.M. Manjaiah, E. Varghese, Polycycl. Aromat. Comp. 34 (2014) 452.

[15] B. Pan, D. Lin, H. Mashayekhi, B. Xing. Environ. Sci. Technol. 42 (2008) 5480.

[16] H.H. Cho, B.A. Smith, J.D. Wnuk, D.H. Fairbrother, W.P. Ball, Environ. Sci. Technol. 42 (2008) 2899.

[17] L. Wang, W. Chen, D. Xu, B.S. Shim, Y. Zhu, F. Sun, L. Liu, C. Peng, Z. Jin, C. Xu, N.A. Kotov, Nano Lett. 9 (2009) 4147.

[18] V.M. Hertz, M. Bolte, H.W. Lerner, M. Wagner, Angew. Chem. Int. Ed. Engl. 54 (2015) 8800.

[19] J. Lenhard, Studies in History and Philosophy of Science Part A 48 (2014) 89.

[20] R. Ahmadi, M. Pirahan-Foroush, AMHSR 12 (2014) 39.

[21] E. Khan, A. Shukla, A Srivastava, Sh. Tandon, P. Tandon, New J. Chem. 2015, DOI: 10.1039/ C5NJ01779C.